Beta Spectra of the Mirror Nuclei*†

ROGER WALLACE AND JASPER A. WELCH, JR.‡
Lawrence Radiation Laboratory, University of California, Berkeley, California
(Received June 4, 1959; revised manuscript received November 20, 1959)

The positron spectra and half lives of all the mirror nuclei ($2Z=A\pm1$) with $19\leqslant A\leqslant 39$ have been systematically measured with a 180°-deflection uniform-magnetic-field spectrometer. The ground-state transition energies were used to compute Coulomb-energy differences between mirror pairs. Deviations of these Coulomb-energy differences from a smooth variation with A are explained by a nuclear shell model using the potential well of an isotropic harmonic oscillator. The data support a symmetry for the proton wave functions characteristic of the state of lowest seniority, with magic-number effects at $A=14$ and 16 as well as $A=8$ and 20. Comparison of the ft values obtained with experimental nuclear magnetic moments gives the following values for the partial coupling constants for the Fermi and Gamow-Teller β interactions: $g_F^2=(1.5\pm0.1)\times10^{-4}$ sec^{-1}, $g_{GT}^2=(2.2\pm0.1)\times10^{-4}$ sec^{-1}. Nuclear radii from μ-mesic atoms, when properly interpreted, are shown to be in agreement with radii deduced from Coulomb energy differences.

I. INTRODUCTION

THE total binding-energy difference between isobars is composed of contributions from nuclear forces, repulsive Coulomb forces between protons, and the neutron-proton mass difference. The nuclear Coulomb energy depends upon the spatial correlations of the several protons in the nucleus, and its value is indicative not only of the general size of nuclei but also of the spatial symmetry of the proton wave functions.[1,2]

In the nuclear shell model with charge-independent nuclear forces, the specific nuclear contribution to the binding energy is the same for pairs of isobars characterized by $2Z=A\pm1$, $2Z=A\pm2$, etc. Thus in these cases we may obtain the Coulomb energy difference by simply correcting the total binding-energy difference for the neutron-proton mass ratio. Experimental total binding-energy differences are obtained from measurements of reaction energy and beta-disintegration energy. In very light nuclei the perturbation of the Coulomb forces somewhat disturbs this nuclear equivalence.

The nuclear species $2Z=A\pm1$ are called mirror nuclei and have been the objects of considerable theoretical[3–7] and experimental[8–11] attention. Very accurate experimental binding-energy data are available for $A\leqslant21$ from reaction-energy measurements. This experiment obtained, from positron-decay disintegration energies, a systematic, accurate set of binding-energy differences throughout the region $19\leqslant A\leqslant39$.[12] The earlier experimental situation was characterized by much disagreement, although several experiments of high precision have been performed recently.

Because nuclear Coulomb energies depend not only upon the size of the nucleus but also upon the overlap of the proton wave functions, nuclear radii deduced from data on mirror nuclei are highly dependent on the model used. Radii obtained from this experiment using a nuclear shell model will be compared with radii from high-energy electron scattering and μ-mesonic atoms.

Values of ft were determined and will be compared with theoretical matrix elements and matrix elements based on measured magnetic moments of the daughter isobars.[4,13] The later comparison gives values for both the Fermi and Gamow-Teller β-decay interaction constants.

II. EXPERIMENTAL PROCEDURE

The radioisotopes were produced by deuteron and proton bombardments with the external beam of the 60-inch cyclotron at Crocker Laboratory, and by proton bombardments at the Lawrence Radiation Laboratory 32-Mev proton linear accelerator, as well as deuteron bombardments with the Van de Graaff injector of that linac.

The beta spectra were measured with a uniform-field 180°-deflection single-focusing spectrometer (Fig. 1). The design was carried out along the lines suggested by Geoffrion and Persico,[14,15] who developed formulae for maximizing transmission for a given resolution. The magnetic field was carefully mapped and calibrated to

* Work performed under the auspices of the U. S. Atomic Energy Commission.
† Based on a dissertation submitted by Captain Welch to the Graduate Division of the University of California in partial fulfillment of the degree of Doctor of Philosophy in Physics.
‡ Captain, U. S. Air Force, presently at the Air Force Special Weapons Center, Kirtland Air Force Base, New Mexico.
[1] E. Feenberg and G. Goertzel, Phys. Rev. **70**, 597 (1946).
[2] B. C. Carlson and I. Talmi, Phys. Rev. **96**, 436 (1954).
[3] K. W. Ford and D. L. Hill, *Annual Review of Nuclear Science* (Annual Reviews, Inc., Palo Alto, 1955), Vol. 5, p. 25.
[4] M. Mayer and J. Jensen, *Elementary Theory of Nuclear Shell Structure* (John Wiley and Sons, Inc., New York, 1955).
[5] O. Kofoed-Hansen, Revs. Modern Phys. **30**, 449 (1958).
[6] Arnell, Dubois, and Almen, Nuclear Phys. **6**, 196 (1958).
[7] P. C. Sood and A. E. S. Green, Nuclear Phys. **4**, 274 (1958).
[8] R. W. King, Revs. Modern Phys. **26**, 327 (1954).
[9] L. J. Lidofsky, Revs. Modern Phys. **29**, 773 (1957).
[10] D. M. Van Patter and W. Whaling, Revs. Modern Phys. **26**, 402 (1954).
[11] D. M. Van Patter and W. Whaling, Revs. Modern Phys. **29**, 757 (1957).
[12] For a full report of this experiment see Jasper A. Welch, Jr., University of California Radiation Laboratory Report, UCRL-3888, August 1957 (unpublished). A preliminary report of results has been presented by R. W. Wallace and J. A. Welch, Jr., in Bull. Am. Phys. Soc. **3**, 206 (1958).
[13] G. L. Trigg, Phys. Rev. **86**, 506 (1952).
[14] E. Persico and C. Geoffrion, Rev. Sci. Instr. **21**, 945 (1950).
[15] C. Geoffrion, Rev. Sci. Instr. **20**, 638 (1949).

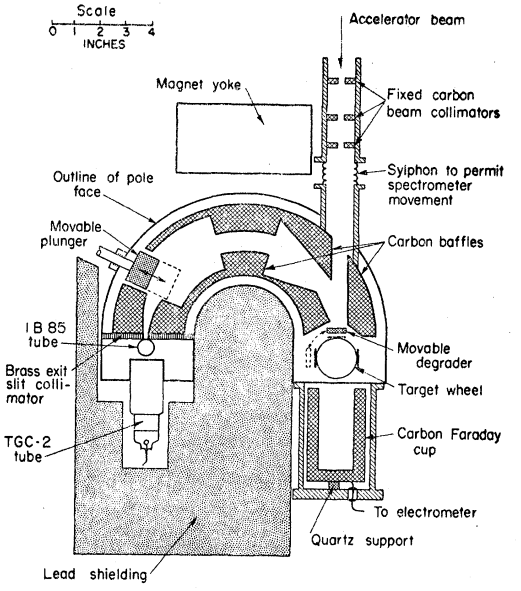

FIG. 1. Schematic cross section through the spectrometer perpendicular to the magnetic field.

0.1% against magnet current with commercial nuclear-magnetic-resonance equipment.

Because of the short half lives encountered, the spectrometer was positioned so that the accelerator's external beam struck a target placed at the entrance of the orbit. To reduce background, everything that would be exposed to direct or scattered beam was fashioned of carbon. The width of the source was determined by beam collimation. Compensation for the deflection of the beam by the spectrometer field was made with a lead-screw traverse for the whole magnet assembly. The energy of the bombarding particle was controlled by a movable carbon degrader interposed just ahead of the target to reduce the beam spread due to multiple scattering in the degrader.

All target materials except aluminum were available in powder form. Targets were prepared by mixing the powder into a dope of styrofoam dissolved in benzene and then allowing the benzene to evaporate. The beam current was collected in a carbon Faraday cup just behind the target. The beam current was fed into an RC circuit whose decay constant equaled that of the activity being investigated. This innovation by Professor W. K. H. Panofsky produces a voltage across the condenser which is at all times proportional to the activity of the target.

The beta particles were detected by two thin-walled gas proportional tubes in coincidence. Scattering (in the counter walls) causes a droop in the coincidence/front-

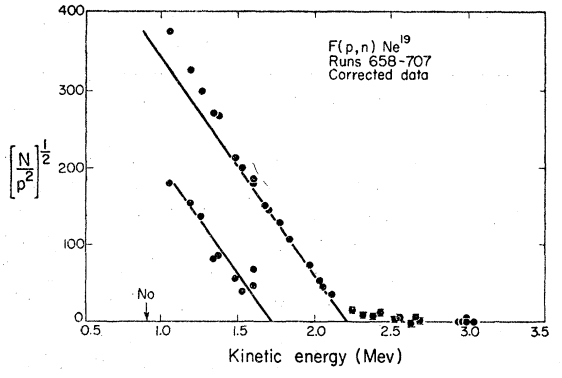

FIG. 2. Kurie plot for the isotope Ne^{19}. The experimental decomposition into branching transitions is shown. Arrows indicate positions of possible branching transitions; Yes above arrow denotes that the spin-parity assignment predicts an allowed transition; No indicates a forbidden transition. (These remarks apply also to Figs. 3 through 12.)

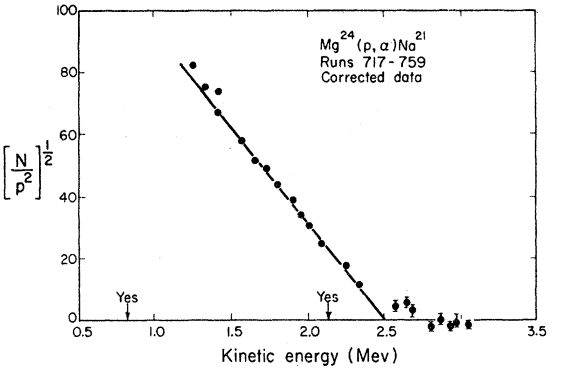

FIG. 3. Kurie plot for Na^{21}.

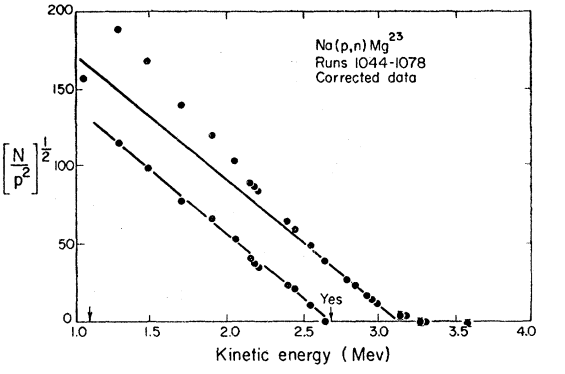

FIG. 4. Kurie plot for Mg^{23}.

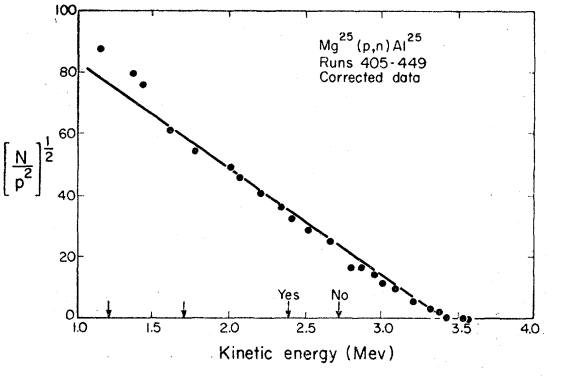

FIG. 5. Kurie plot for Al^{25}.

singles ratio below 1 Mev. We took the front-singles rate as true and corrected the coincidence rate by an empirically determined function.

With the degrader in position the beam was turned on and the target bombarded for three half-lives. At this time the beam was abruptly shut off, and simultaneously the movable degrader was flipped out of the β-particle orbit. The counts were recorded as a function of time after cessation of bombardment with a mechanical tandem-gate apparatus. The first few gates were set at one-half a half-life, and succeeding ones set longer and longer to encompass a total recording time of about twelve half-lives. This bombarding and counting routine was repeated one to ten times at each spectrometer energy (a fixed number for each isotope) to gather 10^4 counts at mid-energy. It was necessary to carry through the routine very systematically in order to maintain good knowledge of the background.

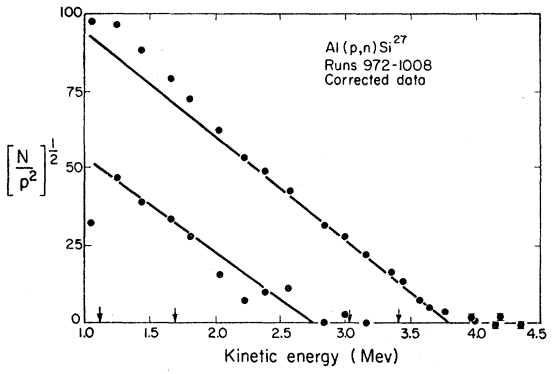

FIG. 6. Kurie plot for Si^{27}.

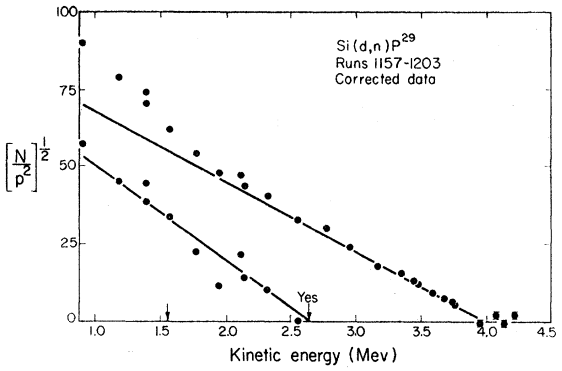

FIG. 7. Kurie plot for P^{29}.

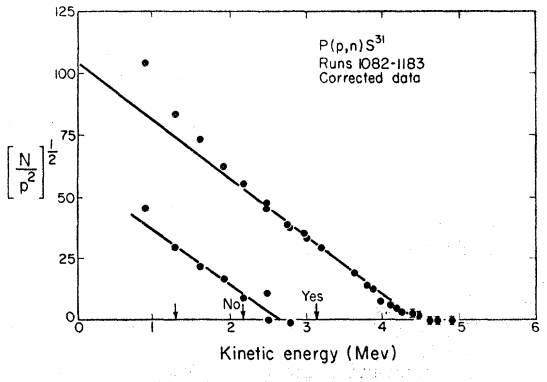

FIG. 8. Kurie plot for S^{31}.

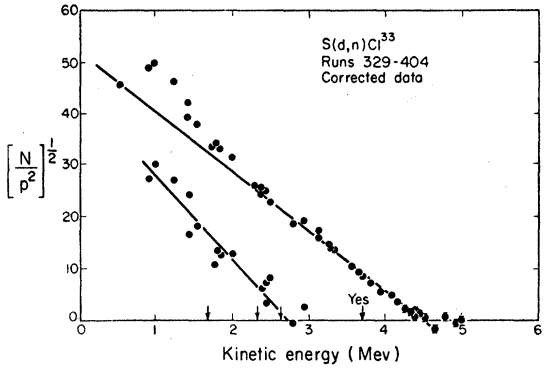

FIG. 9. Kurie plot for Cl^{33}.

A carbon plunger can be inserted into the orbit 30° ahead of the exit slit. This prevents all positrons from reaching the detector, and hence allows direct measurement of all nonorbit background. Runs were also made with a blank target. In all cases subtraction of these background data resulted in a pure activity, and a sum of counts in the first four gates was used as the relative spectral intensity. Unique identification of the observed activity was made from reaction kinetics and approximate knowledge of half-life and end-point energy.

III. EXPERIMENTAL RESULTS

The end-point energies of the spectra were determined by the usual Fermi-Kurie function analysis for allowed spectra, except that, for our low values of Z, the Coulomb-repulsion correction factor changed by at most 2% in the range 1 to 6 Mev and was omitted from the Kurie function as plotted in Figs. 2 through 12.[16]

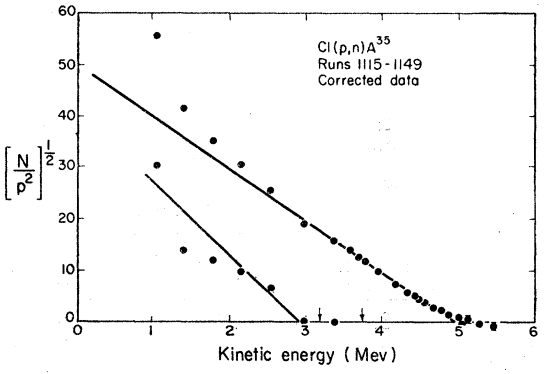

FIG. 10. Kurie plot for A^{35}.

[16] *Tables for the Analysis of Beta Spectra*, National Bureau of Standards, Applied Mathematics, Series 13 (U. S. Government Printing Office, Washington, D. C., 1952), p. 21.

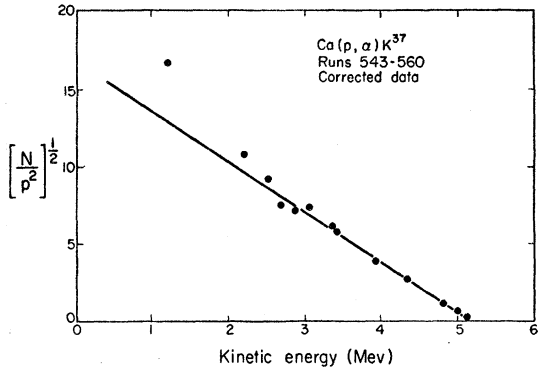

FIG. 11. Kurie plot for K^{37}.

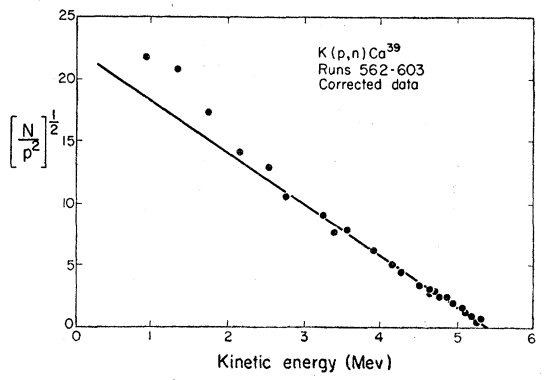

FIG. 12. Kurie plot for Ca^{39}.

The raw Kurie plots exhibited a long tail on the high-energy end extending well beyond what could be accounted for by spectrometer resolution. A review of the data convinced us that it was not due to improper interpretation of the background. From our efficiency versus energy data we determined that the points that correspond to this tail have an efficiency that is characteristic of energies less than 1 Mev, thus indicating that they must have been scattered off the spectrometer walls into the detector. Wong has observed a similar effect.[17] From the shape of the tail, we deduced a tail correction that had the effect of lowering the Kurie-plot intercept 1% to 2% and added no more than 0.1% error to the intercept.

A folded integral over an allowed spectrum with finite resolution and finite source thickness δ revealed that distortion of the Kurie plot is confined to the lower fourth of the energy range and within one base resolution width of the intercept. In addition, the apparent intercept lay, at most $\delta/2$ too low. The experimental results in Fig. 13 indicate a correction of $\delta/4$. We compromised on $\delta/3$, which introduces an error in the intercept of no more than $\delta/10 \cong 0.01$ Mev. All corrections have been applied to Figs. 2 through 12.

The unfolding of branching transitions in these Kurie plots is really somewhat tenuous, owing to counting

[17] C. Wong, Phys. Rev. **95**, 761 (1954).

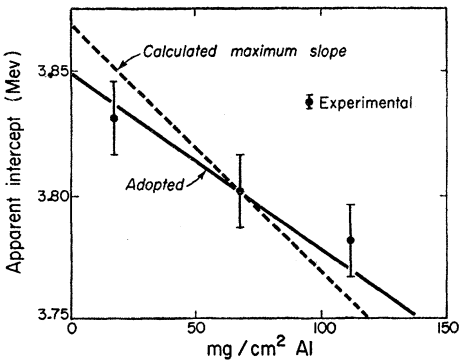

FIG. 13. Source thickness effect. Experimentally observed intercepts for three source thicknesses are shown together with the maximum calculated thickness effect (dashed line) and the adopted correction (solid line).

statistics and our uncertainty in the detection-efficiency correction. Only transitions obeying allowed selection rules ($\Delta J=0$, 1; no parity change) will have a large enough branching ratio to be observed. In most cases correlation can be found with positions of known daughter levels and their spin-parity assignments.[18] For F^{19} we see evidence for a transition to a hitherto unreported state at 0.5 ± 0.2 Mev (see Ne^{21}). For Ne^{21} we do not see a branch to the 0.35-Mev level. Our measurements of $Ne^{19} \rightarrow F^{19}$ and $Na^{21} \rightarrow Ne^{21}$ were taken with comparable source thicknesses, and thus it is hard to see why the F^{19} level is not real; however, it was not observed by either Freeman[19] or Seale.[20] For Mg^{25} we see no branch to the 0.98-Mev level, and no γ rays have been observed from this level.[6] The spin-parity assignment is not absolutely clear-cut but does look reasonable.[21] For S^{33} neither we nor Meyerhof found a branch to the 0.84-Mev level.[22]

From our energy and half-life measurements we have computed *ft* values according to the formulas of Feenberg and Trigg.[23] The correction for branching to excited levels should be less than 5% and has not been made.

The basic magnetic-field measurements are accurate to 0.1% in absolute value; corrections for deviations from a uniform field push the absolute error for the effective field to 0.4% and the relative error to 0.2%. Variations in the position and spatial uniformity of the beam introduce an absolute error no larger than 0.2% in the effective orbit radius. Thus the basic accuracy in the $H\rho$ of the instrument is 0.5% absolutely and 0.3% relatively.

The internal accuracy of individual Kurie plots varied from 0.3% to 1.5% for the ground-state transitions.

[18] P. M. Endt and J. C. Kluyver, Revs. Modern Phys. **26**, 95 (1954).
[19] Joan M. Freeman, Phil. Mag. **1**, 591 (1956).
[20] R. L. Seale, Phys. Rev. **92**, 389 (1953).
[21] J. R. Holt and T. N. Marsham, Proc. Phys. Soc. (London) **66A**, 258 (1952).
[22] W. E. Meyerhof and G. Lindstron, Phys. Rev. **93**, 949 (1954).
[23] E. Feenberg and G. Trigg, Revs. Modern Phys. **22**, 299 (1950).

TABLE I. Data for mirror nuclei. The Coulomb energy difference Δ_1 is obtained as $\Delta_1=E_{max}+1.804$ Mev for β^+, $\Delta_1=E_{max}-0.782$ Mev for β^- and $\Delta_1=E_{max}+0.782$ Mev for K capture. The differences in Δ_1 between adjacent transitions is given in the last column as Δ_2.

Transition	$T_{\frac{1}{2}}$[b]	Ref	E_{max} (Mev)	Ref	ft[a] (sec)	Δ_1 (Mev)	Δ_2 (Mev)
p^1-n^1	11.7±0.3 min.	25	0.782±0.001	26	1230	0.0	···
He^3-H^3	12 yr.	27	0.0186±0.0001	27	1150	0.764±0.001	0.764±0.001
Li^5-He^5	···		proton unstable		···	0.8±0.3	0.04±0.30
Be^7-Li^7	53 day	8	K capture		2340	1.645±0.001	0.85±0.30
B^9-Be^9	···		proton unstable		···	1.852±0.002	0.207±0.002
$C^{11}-B^{11}$	20.11±0.13 min.	6	0.960±0.003	8	3890	2.762±0.003	0.910±0.004
$N^{13}-C^{13}$	597.6±1.8 sec.	6	1.200±0.002	8	4670	3.004±0.002	0.242±0.005
$O^{15}-N^{15}$	123.95±0.50 sec.	28	1.739±0.002	29	4400	3.543±0.002	0.539±0.003
$F^{17}-O^{17}$	66.6±0.5 sec.	6	1.745±0.006	9	2280±100	3.549±0.006	0.006±0.008
$Ne^{19}-F^{19}$	19.5±1.0 sec 17.7±0.1	c 31	2.24±0.01		1800±100	4.04±0.01	0.49±0.02
$Na^{21}-Ne^{21}$	21.6±0.5 sec 23.0±0.2	c 6	2.51±0.02		3800±250	4.31±0.02	0.27±0.02
$Mg^{23}-Na^{23}$	11.9±0.3 sec 12.1±0.1	c 31	3.09±0.01		4900±200	4.89±0.01	0.58±0.02
$Al^{25}-Mg^{25}$	7.3±0.3 sec 7.24±0.03	c 32	3.27±0.03		3600±350	5.07±0.03	0.18±0.03
$Si^{27}-Al^{27}$	4.1±0.2 sec 4.14±0.03	c 31	3.85±0.02		4400±100	5.65±0.02	0.58±0.04
$P^{29}-Si^{29}$	4.2±0.1 sec 4.45±0.05	c 9	3.96±0.02		4800±200	5.76±0.02	0.11±0.03
$S^{31}-P^{31}$	2.58±0.06 sec 2.72±0.02	c 31	4.39±0.03		4800±200	6.19±0.03	0.43±0.04
$Cl^{33}-S^{33}$	2.9±0.1 sec 2.53±0.02	c 32	4.51±0.05		5300±500	6.31±0.05	0.12±0.06
$A^{35}-Cl^{35}$	1.84±0.10 sec 1.83±0.03	c 33	4.93±0.05		5600±400	6.73±0.05	0.42±0.07
$K^{37}-A^{37}$	1.15±0.15 sec 1.23±0.02	c 34	5.15±0.07		4600±500	6.95±0.07	0.22±0.09
$Ca^{39}-K^{39}$	0.89±0.05 sec 0.88±0.01 0.876±0.012	c 35 36	5.43±0.06		4100±300	7.23±0.06	0.28±0.09
$Sc^{41}-Ca^{41}$	0.87±0.05 sec 0.87±0.03	c 8	4.94±0.10	8	2200±250	6.74±0.10	−0.49±0.12

[a] See text for choice of $T_{\frac{1}{2}}$.
[b] Units are years (yr.), days, minutes (min.), and seconds (sec.).
[c] Values from this experiment.

This is compatible with counting-statistics errors, indicating no appreciable contribution from beam monitoring. Every isotope was measured at least twice, and from two to eight spectra were determined during each of nine runs performed over a 10-month period. Many cross checks are thus available, and all determinations are in agreement. The combined relative error from internal fit, source thickness, and $H\rho$ is given in Table I. The entire error in the half life comes from uncertainty in the correct background-counting rate. Our half-life determinations agree with those from other experiments as reported by King.[8] Some recent measurements are[24–38] given in Table I. Where our values are in agreement we have chosen for the ft calculation the half-life with the smallest quoted error. In the cases of P^{29}, S^{31}, and Cl^{33} we favored the smallest value just because unsuspected backgrounds tend to make half-lives appear longer. The errors in the ft values were compounded from absolute

[24] Hunt, Jones, and Churchill, Proc. Phys. Soc. (London) **A67**, 479 (1954).
[25] Soshovskis *et al.*, Geneva, July, (1958).
[26] Li, Whaling, Fowler, and Lauritson, Phys. Rev. **83**, 512 (1951).
[27] L. Friedman and L. G. Smith, Phys. Rev. **109**, 2214 (1958).
[28] J. R. Penning and F. H. Schmidt, Phys. Rev. **105**, 647 (1957).
[29] O. C. Kistner *et al.*, Phys. Rev. **105**, 1339 (1957).
[30] L. J. Lidofsky *et al.*, Bull. Am. Phys. Soc. **2**, 182 (1957).
[31] M. V. Mihailovic and B. Povh, Nuclear Phys. **7**, 296 (1958).
[32] Muller *et al.*, Physica **24**, 577 (1958).
[33] O. C. Kistner *et al.*, Phys. Rev. **104**, 154 (1956).
[34] F. Schweizer, Phys. Rev. **110**, 1414 (1958).
[35] O. C. Kistner and B. M. Rustad, Phys. Rev. **112**, 1972 (1958).
[36] J. E. Cline and P. R. Chagnon, Bull. Am. Phys. Soc. **3**, 206 (1958).
[37] Elbek, Madison, and Nathan, Phil. Mag. **46**, 663 (1955).
[38] C. R. Sun and B. T. Byron, Phys. Rev. **109**, 109 (1958).

TABLE II. Data from this experiment compared with values obtained by reaction kinetics and beta spectra.

Transition	Beta spectra Ref	Method[a]	$\Delta_1=E_{\beta^+}+1.804$ (Mev)	Q values Ref	Method	$\Delta_1=-Q(p,n)$ or $\Delta_1=Q(d,p)-Q(d,n)$ (Mev)	This experiment $\Delta_1=E_{\beta^+}+1.804$ (Mev)
$Ne^{19}-F^{19}$	8	S	3.98±0.03	10	(p,n)	4.039±0.004	4.04±0.01
	8	A	4.1±0.1				
$Na^{21}-Ne^{21}$	8	S	4.30±0.03	10	$(d,p;d,n)$	4.70±0.05	4.31±0.02
	8	Scin	4.3±0.1				
$Mg^{23}-Na^{23}$	8	Scin	4.75±0.07	10	(p,n)	4.88±0.01	4.89±0.01
	8	CC	4.62±0.14				
$Al^{25}-Mg^{25}$	24	A	4.97±0.15	11	(p,n)	5.084±0.024	5.07±0.03
	37	S	5.04±0.03	10	$(d,p;d,n)$	5.02±0.06	
$Si^{27}-Al^{27}$	9	Scin	5.62±0.04	11	(p,n)	5.593±0.009	5.65±0.02
	8	CC	5.34±0.10				
	8	CC	5.54±0.19				
$P^{29}-Si^{29}$	9	Scin	5.62±0.04	10	$(d,p;d,n)$	5.96±0.04	5.76±0.02
	8	S	5.749±0.010				
	8	Scin	5.7±0.2				
$S^{31}-P^{31}$	9	Scin	6.22±0.03	10	(p,n)	6.06±0.20	6.19±0.03
	8	CC	5.67±0.07				
$Cl^{33}-S^{33}$	8	Scin	6.0±0.2	10	$(d,p;d,n)$	6.17±0.04	6.31±0.05
$A^{35}-Cl^{35}$	9	S	6.76±0.05			···	6.73±0.05
	8	CC	6.21±0.09				
$K^{37}-A^{37}$	38	S	6.90±0.07			···	6.95±0.07
$Ca^{39}-K^{39}$	9	Scin	7.38±0.04			···	7.23±0.06
	35	S	7.290±0.025				
$Sc^{41}-Ca^{41}$	8	CC	6.74±0.08	11	$(d,p;d,n)$	6.74±0.010	···

[a] The notation S denotes that a magnetic spectrometer was used, A denotes absorption, CC denotes cloud chamber and Scin denotes a crystal scintillator.

energy and half-life errors, based on $ft\sim E^5t$ for this region of energies.

Table II presents some Q-value measurements together with previous β-spectra measurements and the results of this experiment. We have chosen to use the Coulomb-energy differences for comparison. These are obtained from β decay as $\Delta_1=E_{\max}+1.804$ Mev for β^+, from (p,n) thresholds as $\Delta_1=Q(p,n)$; and from difference of (d,n) and (d,p) reaction energies as $\Delta_1=Q(d,p)-Q(d,n)$, where the two reactions lead from a common nucleus to the members of a mirror pair. We agree with all the values from (p,n) reactions except at $A=27$, where our value is slightly too high for the quoted errors to overlap. For the deuteron-reaction differences, our values are higher than 2 and below 2, and beyond the reported experimental errors in all cases. However, we should point out the excellent agreement of this method and the β-energy determination for Sc^{41}.

TABLE III. Values of the alternation parameter obtained from experimental values of Δ_2 compared with theoretical values based on various coupling schemes in the C-T model.

Orbital for odd nucleon	Alternation parameter, $(a-b)/(a+b)$ LS in state of lowest seniority	jj in state of lowest seniority	LS averaged over spin	This experiment
$Od_{5/2}$	0.44	0.55	0.83	0.41±0.12
$Od_{3/2}$	0.44	0.40	0.83	0.62±0.25

IV. DISCUSSION

The classical formula for the Coulomb energy of Z protons distributed uniformly throughout a spherical volume of radius R is

$$E_c=(3/5)Z(Z-1)e^2/R, \quad (1)$$

and the Coulomb energy difference between the mirror pair $(Z+1)$, Z is

$$\Delta_1(Z)\equiv E_c(Z+1)-E_c(Z)=(6/5)e^2Z/R. \quad (2)$$

Assuming further that $R=r_0A^{\frac{1}{3}}$, we find that $\Delta_2(Z)\equiv\Delta_1(Z+1)-\Delta_1(Z)$ will be a smoothly varying function of Z.

One defect in this model is the tacit assumption that the protonic charge carried away in the β decay comes uniformly from over the entire charge distribution. The nuclear shell model clearly implies that to the contrary the "disappearing" proton comes from a definite state with a nonuniform probability distribution. If the charge density remains constant so that the charge contained in the outermost spherical shell is carried away, we calculate a reduction in Δ_1 of 15% over that of Eq. (2). Because of the exclusion principle, the total proton wave function must be antisymmetric in the exchange of two particles, i.e., the protons appear to avoid one another. Simply placing the protons in a cubic lattice leads to a 15% reduction in the Coulomb energy over that given by Eq. (1). Cooper and Henly obtain a

12% reduction for the Hartree approximation to antisymmetrization.[39] The grouping of protons into space-symmetric, spin-antisymmetric pairs implies that the Δ_1 for odd $Z \rightarrow$ even Z should be relatively smaller than for even $Z \rightarrow$ odd Z; hence Δ_2 should be an alternating function of Z.

Following the work of Feenberg and Goertzel,[1] Carlson and Talmi[2] (henceforth denoted by C-T) have developed a detailed theory of Coulomb energies with a nuclear shell model. On the basis of lowest seniority for mirror-nuclei ground states, they obtain $\Delta_2 = a + (-1)^{Z'+1} b$, where Z' is the number of protons outside a closed shell. Now a and b do not depend on Z'; they do depend upon the choice of jj or LS coupling, the l or j of the level being filled, and the radial form of the wave functions. The Coulomb energy is calculated as a perturbation to first order by the use of jj coupling and single-particle wave functions that are stationary states of the well of an isotropic harmonic oscillator. They find $\Delta_1 = \xi(A)\epsilon$, where $\xi(A)$ can be evaluated analytically and ϵ is an energy characteristic of the oscillator force constant. This force constant represents the average nuclear force on the Z' protons outside closed shells.

From Fig. 14 we see that, outside the $Op_{\frac{3}{2}}$ shell, experimental values of ϵ are remarkably uniform within shells. Furthermore the values are in good agreement with those obtained by Talmi and Theiberger (henceforth denoted by T-T) when they fit a five-parameter theoretical binding-energy formula to all known light nuclei.[40]

The uniformity of alternation of Δ_2 in the $d_{\frac{5}{2}}$ shell and the interruption of the quantitative uniformity at the beginning of each shell above $P_{\frac{3}{2}}$ is shown in Fig. 15. In Table III are presented the average experimental values of the alternation parameter $(a-b)/(a+b)$ together with the computed values (by C-T) for jj and LS coupling for the state of lowest seniority, as well as for an average over all states in LS coupling having the same spin. The $d_{\frac{5}{2}}$ data favor the state of lowest seniority, while the $d_{\frac{3}{2}}$ data are really too inaccurate to discriminate. It is not clear from C-T whether these values for $(a-b)/(a+b)$ would change radically for another type of potential well, although the work of Jancovinci[41] suggests they would not.

The C-T model also gives a relationship between the radius constant of the charge distribution and the Coulomb-energy difference, $\Delta_1 r_0 = \sigma(A)$, where r_0 is defined for the equivalent uniform distribution as $r_0 A^{\frac{1}{3}} = (5/3)^{\frac{1}{2}} \langle r^2 \rangle^{\frac{1}{2}}$, and $\sigma(A)$ can be evaluated analytically. It should be pointed out that the model itself implies that r_0 decreases uniformly throughout a shell if ϵ is constant. The experimental values of r_0 (see Fig. 16) are substantially in agreement with electron-scattering experiments[42] except for the point at $A=24$. This is a region

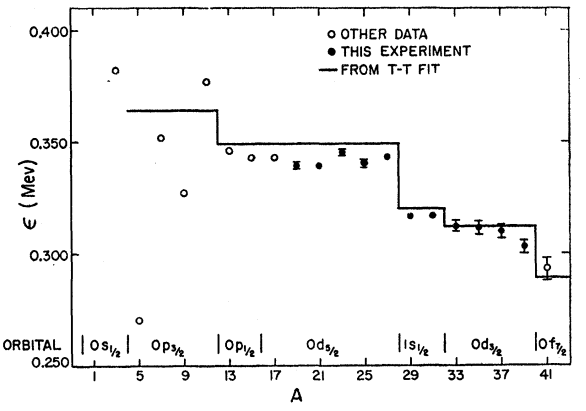

FIG. 14. Characteristic Coulomb energy of the harmonic-oscillator well, ϵ, *versus* A and orbital of the odd nucleon. This energy is defined by $\epsilon = e^2(\tau/\pi)^{\frac{1}{2}}$, $V(r) = \hbar\omega\tau r^2$. Note the large alternations in the $Op_{3/2}$ shell, indicating break-down of the model for extremely small A. The value of ϵ is remarkably constant within higher shells, however. Values of ϵ deduced from a fit of the total binding energies of all known isotopes are shown for comparison.[40]

where evidences for nonspherical nuclei have been found. Now, the electron-scattering experiments are very sensitive to the shape of the charge distribution near the surface, and any deformation would enter into the average fuzziness of the surface to first order. The Coulomb energy necessarily depends on deformation to second order. Thus we might expect the model to give detailed explanation of energies while being insensitive to actual departures from sphericity.

The radii from μ-meson x ray determinations are consistent with a constant value for r_0 of 1.2 fermis, but accurate measurements are confined to the region above $A=51$. The C-T model, when normalized either to the mirror difference at $A=41$ or the fit of T-T, predicts $r_0=1.2$ for $A=51$. Thus the stated disagreement[3] between the μ-mesonic atom radii and those from mirror

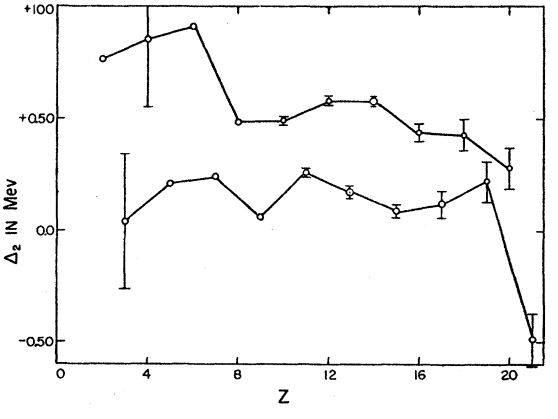

FIG. 15. Second differences with respect to Z of the Coulomb-energy contribution to the total binding energy. The ordinate is defined as $\Delta_2(Z) = \Delta_1(Z+1) - \Delta_1(Z)$, where $\Delta_1(Z) = E_c(Z+1) - E_c(Z)$. Note the odd-even effect throughout and the quantitative interruptions of this effect after $Z=8$, 14, 16, and 20.

[39] L. N. Cooper and E. M. Henly, Phys. Rev. **92**, 801 (1953).
[40] I. Talmi and R. Theiberger, Phys. Rev. **103**, 718 (1956).
[41] B. G. Jancovici, Phys. Rev. **95**, 389 (1954).
[42] Richard H. Helm, Phys. Rev. **104**, 1466 (1956).

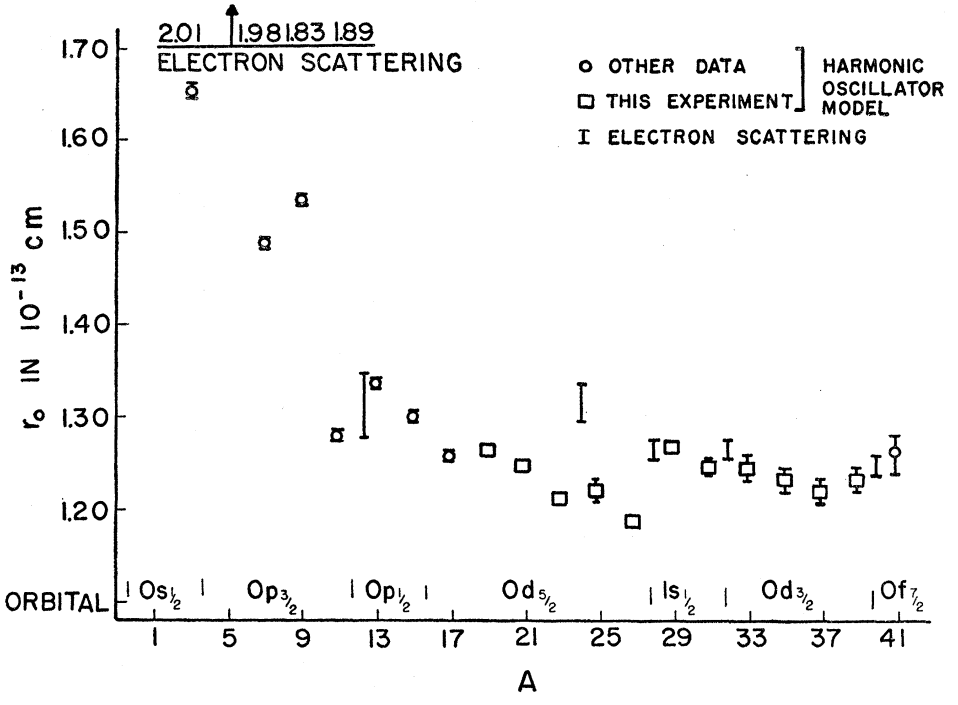

FIG. 16. Root mean square radius constant versus A and orbital of odd nucleon. Values shown are based on a nuclear shell model using harmonic-oscillator wave functions.[2] Electron-scattering results are shown for comparison.

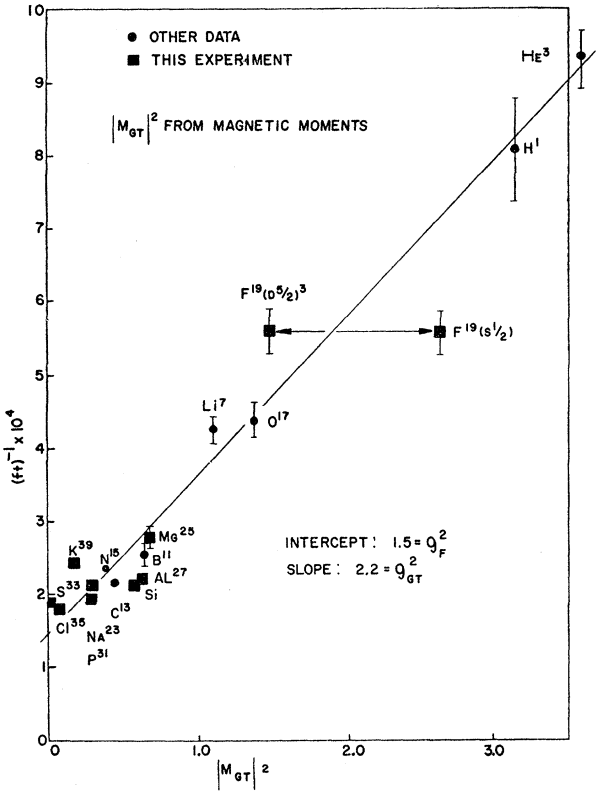

FIG. 17. Experimental values of $(ft)^{-1}$ versus values of the Gamow-Teller matrix element calculated from experimental nuclear magnetic moments.

nuclei disappears when they are compared with a suitable theory in the correct mass-number region.

Following the method of Wilkinson[43] we have calculated the position of the $T=1$ energy levels in the nuclei $2Z=A$ from our mirror pair mass differences. With the exception of the level for $A=38$, the agreement with observation is excellent. The average from $A=22$ to 34 of $(E_{\text{calc}}-E_{\text{obs}})$ is $+0.053\pm0.074$ Mev. Wilkinson shows that this implies that the $n-p$ bond is 1.5% $\pm2.5\%$ stronger than the $n-n$ bond.

The comparative half-life ft can be expressed as

$$(ft)^{-1}=g_F^2|M_F|^2+g_{GT}^2|M_{GT}|^2, \tag{3}$$

where g_F^2 and g_{GT}^2 are the natural constants for the Fermi and Gamow-Teller couplings and $|M_F|^2$ and $|M_{GT}|^2$ denote the respective matrix elements. For mirror transitions we have $|M_F|^2=1$ on the basis of any reasonable coupling scheme. Thus a plot of $(ft)^{-1}$ versus $|M_{GT}|^2$ should be a straight line with intercept g_F^2 and slope g_{GT}^2. Theoretical values of $|M_{GT}|^2$ do not produce such a result.[13] If the assumptions are made that jj coupling is in operation for charge-independent nuclear forces, Jensen and Mayer[4] have shown that for mirror nuclei there exists a definite relationship between $|M_{GT}|^2$ and the nuclear magnetic moment, μ:

for $j=l+\frac{1}{2}$

$$|M_{GT}|^2=\frac{J+1}{J}\left|\frac{2\mu-(J/j)(l+0.88)}{4.70+l}\right|^2,$$

[43] D. H. Wilkinson, Phil. Mag. **1**, 1030 (1956).

for $j=l-\frac{1}{2}$

$$|M_{GT}|^2=\frac{J+1}{J}\left|\frac{2\mu-(J/j+1)(l+0.12)}{3.70-l}\right|^2.$$

Using these formulas we have computed $|M_{GT}|^2$ from the experimental magnetic moments and compared them with the experimental *ft* values by means of Eq. (3) in Fig. 17. A least-squares fit gives the values $g_F^2=(1.5\pm0.1)\times10^{-4}$ sec^{-1} and $g_{GT}^2=(2.2\pm0.1)\times10^{-4}$ sec^{-1}, in good agreement with the work of Gerhart,[44] Blatt,[45] and Kofoed-Hansen.[46] An equally good fit to the same values of g^2 (with the exception of the point for He^3) can be obtained from the semiempirical matrix elements of Trigg,[13] who adjusted his *LS* matrix elements according to deviations of the experimental magnetic moment from corresponding computed values.

[44] J. R. Gerhart, Phys. Rev. **95**, 288 (1954).
[45] John M. Blatt, Phys. Rev. **89**, 83 (1953).
[46] A. Winther and O. Kofoed-Hansen, Kgl. Danske Videnskab. Selskab, Mat-fys. Medd. **27**, No. 14 (1953).

ACKNOWLEDGMENTS

This research was suggested by Professor Luis Alvarez, and the authors gratefully acknowledge his support and advice during its completion. They also wish to thank Don Gow, Robert Layman, Dr. Selig Kaplan, Robert Cence, H. Wade Patterson, and many others throughout the laboratory for their contributions to the experimental program.

PHYSICAL REVIEW VOLUME 117, NUMBER 5 MARCH 1, 1960

Fission Cross Section of Plutonium-242*

DANIEL K. BUTLER
Argonne National Laboratory, Lemont, Illinois
(Received September 21, 1959)

The cross section for neutron induced fission of Pu^{242} has been measured between 0.1 and 1.7 Mev. The measurement was made by determining the ratio of the Pu^{242} fission cross section to that of U^{235} using a back to back gas scintillation counter.

APPARATUS AND EXPERIMENTAL METHOD

THE ratio of the neutron induced fission cross section of Pu^{242} to that of U^{235} has been measured. The known[1] fission cross section of U^{235} was used to determine the fission cross section of Pu^{242}.

The details of the gas scintillation counter are shown in Fig. 1. The fissionable deposits were supported at the center of a thin walled (0.010 in.) stainless steel cylinder. Flanges were welded to the ends of the cylinder so that Vycor windows could be sealed on with lead gaskets. The gas filling mixture was 1.7% N_2 and 98.3% A at a total pressure of two atmospheres. This mixture was determined to give maximum α-particle pulse height for the particular counter geometry.

The fissionable samples were prepared by electrodeposition. The Pu^{242} used[2] was sample No. 2 of reference 2. The mass (230 μg) of this sample was determined by a mass spectrographic measurement of its isotopic composition combined with α counting. The mass of the uranium sample (4.73 mg U^{235}) was determined in its preparation by quantitative deposition.

The measurements were made by placing the counter with the centers of the deposits $3\frac{1}{2}$ in. from a lithium target. Neutrons were produced in the target by the $Li^7(p,n)Be^7$ reaction using protons from a 3-Mev Van de Graaff electrostatic accelerator. The energy of the neutrons was determined by measuring the energy of the protons with an electrostatic analyzer. The lithium targets used were about 30-kev thick at the (p,n) threshold and the energy spread due to geometry was less than 20 kev. The total combined neutron energy spread at all energies was always less than 60 kev. In order to correct for absorption in the sample backing foils the deposits were placed at an angle of 30° to the neutron flux with the flux alternately incident on the plutonium and the uranium samples.

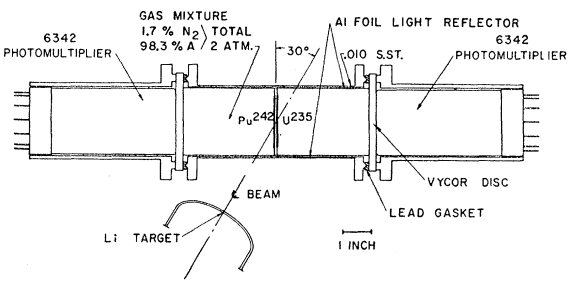

FIG. 1. Back to back gas scintillation counter.

* This work was performed under the auspices of the U. S. Atomic Energy Commission.
[1] *Neutron Cross Sections*, compiled by D. J. Hughes and R. Schwartz, Brookhaven National Laboratory Report BNL-325 (Superintendent of Documents, U. S. Government Printing Office, Washington, D. C., 1958), second edition.
[2] Mech, Diamond, Studier, Fields, Hirsch, Stevens, Barns, Henderson, and Huizenga, Phys. Rev. **103**, 340 (1956).